

New Phytologist Supporting Information

Hidden genetic variation in plasticity provides the potential for rapid adaptation to novel environments

Greg M. Walter, James Clark, Delia Terranova, Salvatore Cozzolino, Antonia Cristaudo, Simon J. Hiscock and Jon R. Bridle (Correspondence to: greg.walter@monash.edu)

Accepted 2 January 2023

Contents:

Table S1 Sampling locations

Fig. S1 Map of experiment and sampling locations

Fig. S2 Genotype choice for gene expression analysis

Fig. S3 Visualizing variation in gene expression across genotypes, clones and elevation

Table S2 Additive genetic (co)variance matrix for absolute fitness across elevation

Table S3 Sire breeding values for fitness at 2,000 m

Table S4 Multiple regression to quantify phenotype-fitness associations

Fig. S4 Histogram of differentially expressed genes

Table S5 Significant gene ontology terms for differentially expressed genes

Table S6 Differentially expressed genes for leaf development and shape in *Arabidopsis*

Fig. S5 Expression changes in the genes that function in *Arabidopsis* leaf morphology

Methods S1 Comparing fitness as the number of flowers versus seed production

Methods S2 RNA extraction, sequencing and transcriptome assembly

Methods S3 Contribution of site variance to estimates of genetic variance

Methods S4 Relating phenotypic traits to the elevational gradient

Table S1: Location of sampled individuals of *S. chrysanthemifolius* used as the parental generation for the crossing design used in the glasshouse. See **Fig. S1** for a map of locations.

Site	Elevation	Latitude	Longitude	# Sires	# Dams
Bonnano	790 m	37°38'24.92"N	15° 2'50.80"E	9	10
Cacciola	680 m	37°37'31.32"N	15° 3'26.71"E	6	6
Poggofelice	526 m	37°39'44.31"N	15° 5'48.55"E	6	5
Spina	730 m	37°39'19.27"N	15° 4'30.92"E	9	10
Treecastagni	571 m	37°36'46.67"N	15° 4'29.64"E	6	5
Totals				36	36

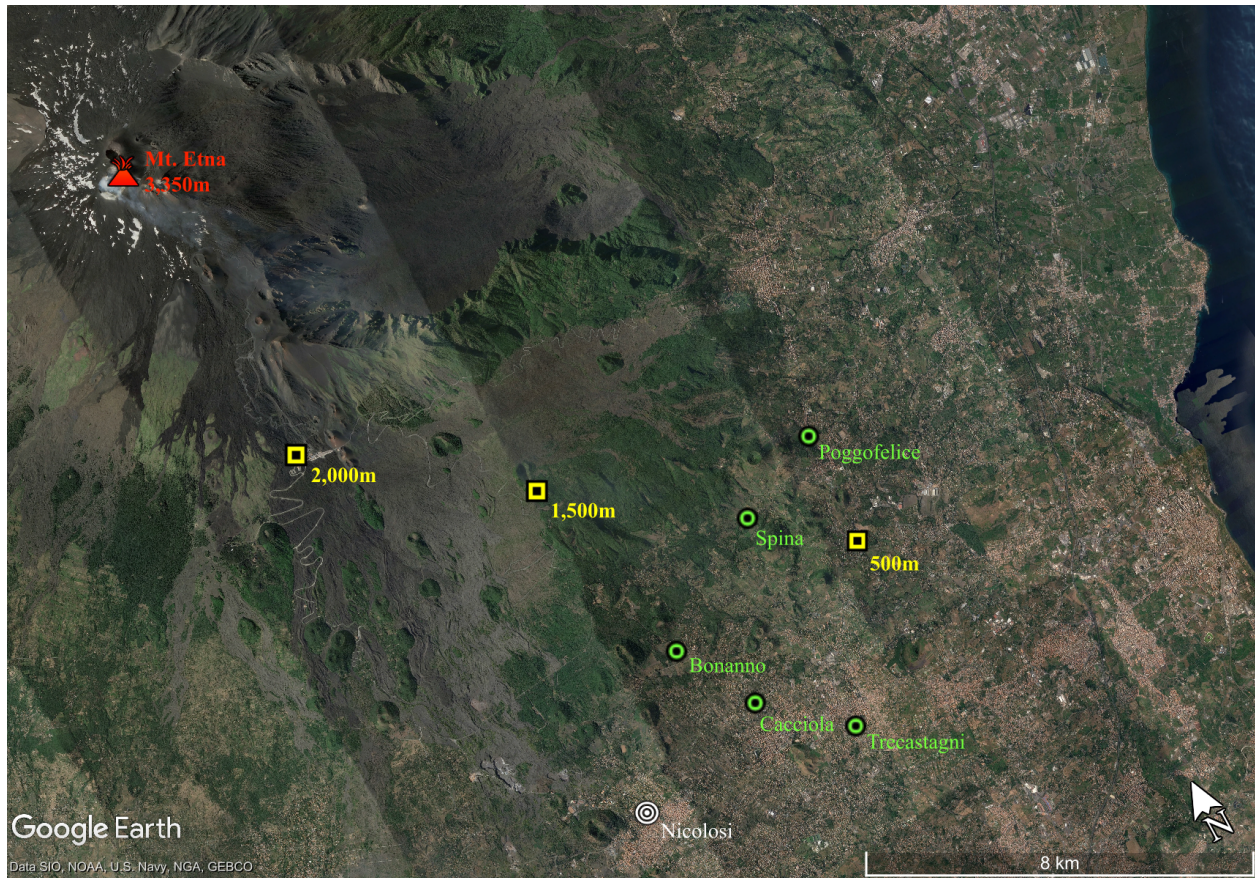


Fig. S1 Map of the experiment. Transplant sites (yellow squares) lie along a south-eastern transect. Sites where genotypes for the parental generation were sampled are represented by green circles. See **Table S1** for coordinates.

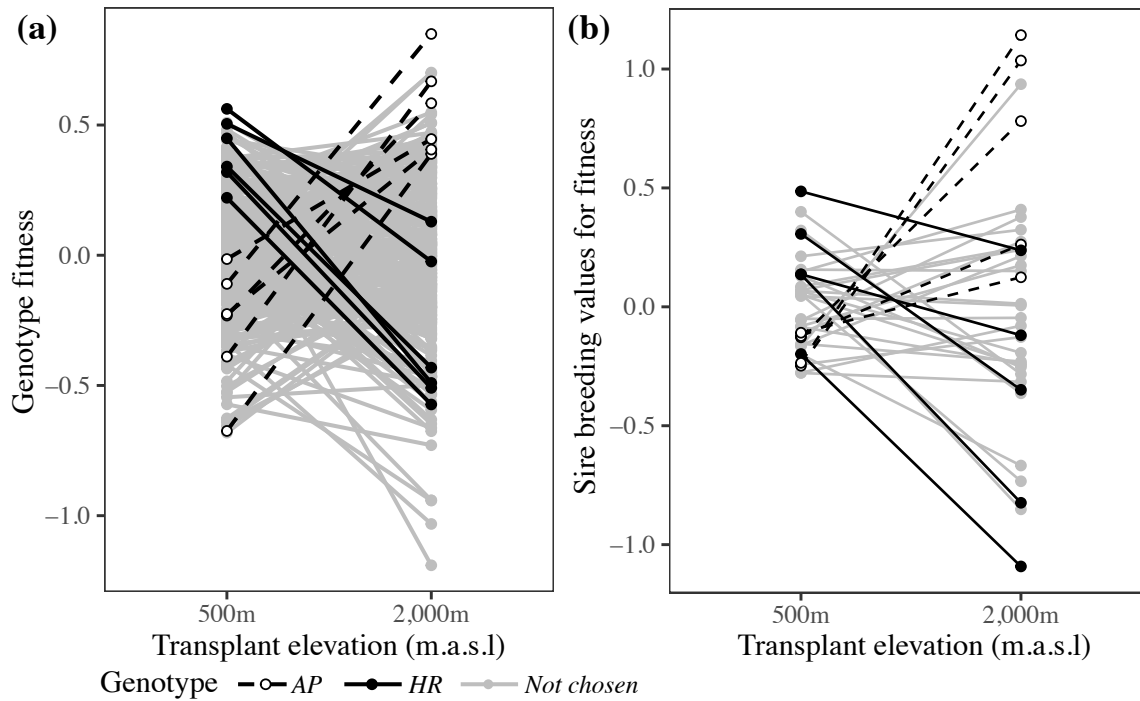


Fig. S2 Selection of genotypes of *S. chrysanthemifolius* based on their fitness response between elevational extremes, calculated using equation 1. **(a)** Chosen genotypes were based on changes in relative fitness from the home site (500 m) to outside the range (2,000 m) for all offspring of the crossing design. Unfilled circles and broken lines represent the *AP* (*Adaptive Potential*) genotypes, and filled circles and solid lines represent the *HR* (*Home Range*) genotypes, that were chosen for the gene expression analysis. Gray lines and circles represent the remaining genotypes from the crossing design that were not chosen. **(b)** The 12 genotypes chosen for the gene expression analysis were from 10 sires that also showed large changes in relative fitness. Therefore, genotypes chosen for the study of differential expression also represented additive genetic variance in fitness.

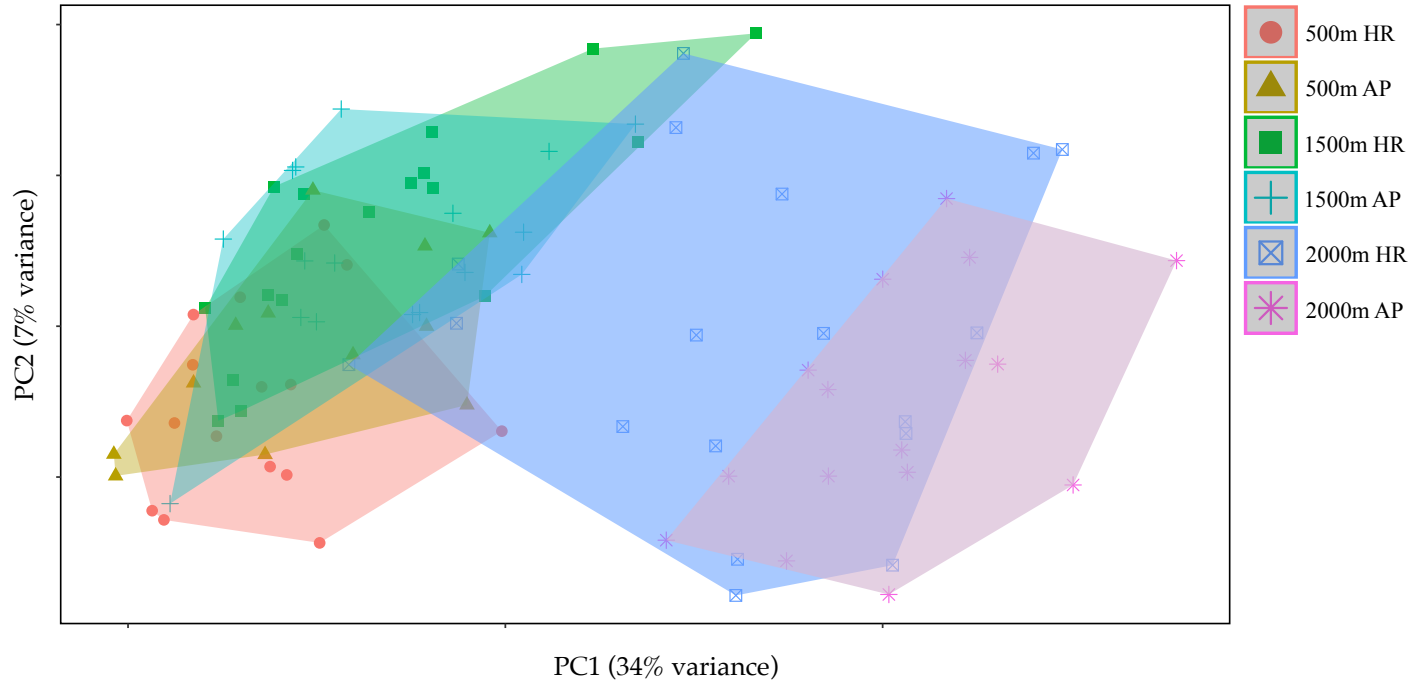


Fig. S3 Variation in gene expression among the 98 samples for the 12 selected genotypes of *S. chrsyanthemifolius*. Individuals represent clones belonging to one of 12 genotypes that included 6 high fitness *AP* (for *Adaptive Potential*) and 6 low fitness *HR* (for *Home Range*) genotypes. Genotypes are colored according to transplant site (meters above sea level) and genotype (*AP* and *HR*).

Table S2: The additive genetic covariance matrix for absolute fitness. The diagonal contains the additive genetic variance in absolute fitness at each elevation. Genetic covariances between elevations are presented above the diagonal, and the genetic correlations between elevations are presented below the diagonal. Numbers in parentheses denote 90% HPD intervals.

	500 m	1,500 m	2,000 m
500 m	732.076 (0, 1530.369)	127.475 (-212.034, 511.423)	-14.797 (-127.7, 95.091)
1,500 m	0.18 (-0.42, 0.88)	504.409 (0, 1123.95)	54.921 (-24.666, 166.955)
2,000 m	-0.1 (-0.76, 0.49)	0.35 (-0.18, 0.86)	58.359 (6.252, 112.801)

Table S3 Breeding values for each sire arranged in order of fitness at 2,000 m. Colors represent the different source sites from where the parental sires were sampled.

Site	Sire	BLUP for fitness at 2,000 m
Trecastagni	43	-1.0888447
Poggofelice	38	-0.8715609
Trecastagni	7	-0.813119
Cacciola	67	-0.7222338
Poggofelice	19	-0.6791872
Trecastagni	62	-0.3871309
Poggofelice	26	-0.3526613
Trecastagni	49	-0.2990977
Cacciola	51	-0.2676762
Poggofelice	32	-0.2585369
Bonnano	44	-0.2393247
Spina	15	-0.2377734
Spina	56	-0.222774
Cacciola	31	-0.1794271
Spina	45	-0.1316659
Cacciola	21	-0.1168628
Spina	50	-0.0840763
Trecastagni	69	-0.0503502
Cacciola	14	0.01473255
Spina	8	0.01862107
Spina	68	0.1276029
Bonnano	33	0.16324835
Spina	2	0.16472873
Poggofelice	61	0.21531416
Bonnano	20	0.23538244
Bonnano	37	0.24987902
Bonnano	9	0.2545542
Poggofelice	57	0.26270505
Bonnano	39	0.28823247
Bonnano	13	0.3598893
Cacciola	1	0.37181873
Bonnano	25	0.42108935
Trecastagni	3	0.78915086
Bonnano	55	0.94840234
Spina	27	1.04734513
Spina	63	1.12295376

Table S4 Summary statistics for the multiple regressions applied to each transplant site. R^2 values are provided for the fixed effects alone (marginal) and when taking into account both fixed and random effects that include environmental block and genotype within the crossing design (conditional). Statistical tests for significant association between traits and fitness were conducted using log-likelihood ratio tests (χ^2 = Chi-square statistic for the likelihood ratio test), which show that leaf traits were significantly associated with fitness at all transplant elevations.

Elevation	Trait	Estimate	95% CI	χ^2	P-value
500 m	Intercept	5.245	5.027, 5.463		
Marginal $R^2=10.08\%$	1. Leaf area (mm ²)	0.014	0.006, 0.022	11.58	0.00067
	2. Leaf complexity (perimeter ² /area)	0.137	0.121, 0.153	280.41	<0.0001
Conditional $R^2=98.33\%$	3. Number of indents (# / perimeter)	-0.609	-0.644, -0.574	1166.61	<0.0001
	4. Specific Leaf Area (SLA, mm ² / μ g)	0.545	0.515, 0.574	1327.72	<0.0001
	5. Flavonol content (light absorbance)	-0.152	-0.168, -0.136	360	<0.0001
1,500 m	Intercept	4.927	4.479, 5.376		
Marginal $R^2=6.86\%$	1. Leaf area	0.119	0.108, 0.131	402.62	<0.0001
	2. Leaf complexity	0.255	0.235, 0.276	597.24	<0.0001
Conditional $R^2=98.95\%$	3. Number of indents	-0.312	-0.341, -0.284	458.1	<0.0001
	4. SLA	0.143	0.118, 0.168	123.28	<0.0001
	5. Flavonol content	0.115	0.1, 0.13	221.45	<0.0001
2,000 m	Intercept	2.388	1.987, 2.789		
Marginal $R^2=15.37\%$	1. Leaf area	0.286	0.238, 0.334	134.33	<0.0001
	2. Leaf complexity	0.23	0.18, 0.279	81.39	<0.0001
Conditional $R^2=94.67\%$	3. Number of indents	-0.745	-0.825, -0.666	345.94	<0.0001
	4. SLA	0.939	0.88, 0.999	943.24	<0.0001
	5. Flavonol content	0.159	0.125, 0.193	83.44	<0.0001

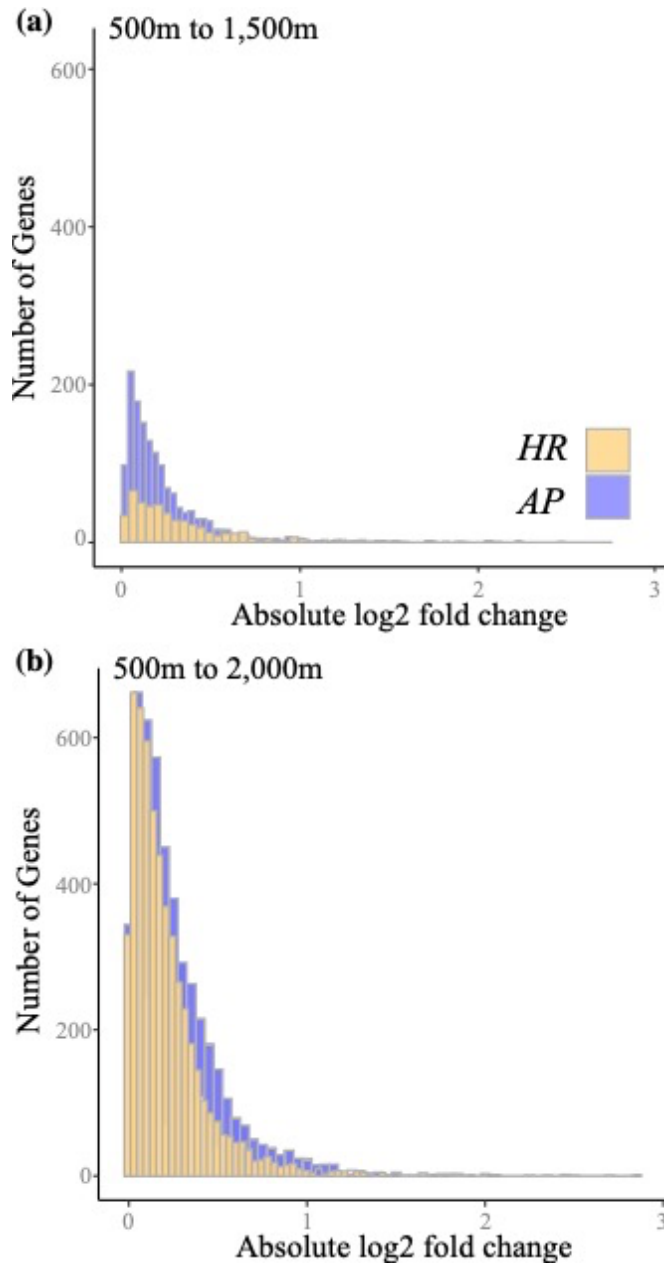


Fig. S4 The strength of differential expression for *Home Range HR* (orange) vs *Adaptive Potential AP* (blue) genotypes of *S. chrysnathemifolius*. **(a)** Within the native range (500-1,500 m), *AP* genotypes differentially express more genes compared to *HR* genotypes. **(b)** Outside the native range (500-2,000 m), both genotypes differentially express more genes, with *AP* genotypes showing greater magnitude of expression changes.

Table S5 Significantly enriched Gene Ontology (GO) terms between the two sets of genotypes of *S. chrysanthemifolius* (*AP* and *HR*) at 2,000 m. Significance defined as p-value < 0.05 following both a Kolmogorov Smirnov (KS) test and Fisher's exact test (Fisher's).

<i>Gene Ontology Term</i>	<i>Gene Ontology Description</i>	p-value (KS)	p-value (Fisher's)
GO:0009765	Photosynthesis, light harvesting	7.6e-7	1.3e-8
GO:0018298	Protein-chromophore linkage	1.6e-6	2.2e-6
GO:0009768	Photosynthesis, light harvesting in PSI	3.9e-6	0.0006
GO:0071555	Cell wall organization	2.5e-6	0.0018
GO:0019684	Photosynthesis, light reaction	0.0005	1.2e-5
GO:0010143	Cutin biosynthetic process	0.001	0.0008
GO:0009809	Lignin biosynthetic process	0.003	0.03
GO:0009409	Response to cold	0.004	0.0008
GO:0010166	Wax metabolic process	0.005	0.02
GO:0009831	Plant-type cell wall modification	0.007	0.01
GO:0042335	Cuticle development	0.008	1.2e-5
GO:0006949	Syncytium formation	0.009	0.02
GO:0009807	Lignan biosynthetic process	0.014	0.006
GO:0045493	Xylan catabolism	0.024	0.003
GO:0009644	Response to high light intensity	0.024	0.007
GO:0015976	Carbon utilisation	0.025	0.004

Table S6. Genes identified from the *Arabidopsis* database tagged with the keywords “Leaf development”, “Leaf morphogenesis”, “Leaf shape”, “Leaf margin” and “Leaf lamina” that were differentially expressed in *AP* and *HR* genotypes of *S. chrysanthemifolius* between 500 and 2,000m.

TAIR locus	Name	Keyword	<i>S. chrys. locus</i>	Adj. p-value (500 vs 2000m)	
				AP	HR
AT3G22200	POP2	Leaf development	DN13080_c2_g1_i11	1.5E-06	9.8E-12
			DN13080_c2_g2_i5	4.0E-02	-
AT4G02570	AXR6	Leaf development	DN1738_c0_g1_i1	1.0E-02	9.4E-03
			DN3264_c0_g1_i1	2.0E-02	3.6E-04
AT1G53310	PEPC1	Leaf development	DN1761_c0_g1_i3	5.0E-10	1.6E-10
			DN1761_c0_g1_i7	2.7E-10	7.4E-09
AT2G37860	RE	Leaf development	DN5928_c0_g1_i3	6.4E-03	2.0E-04
AT1G14280	PKS2	Leaf development	DN3650_c0_g1_i2	6.9E-08	-
AT2G42200	SPL9	Leaf development	DN12076_c0_g1_i2	2.0E-02	2.0E-03
AT3G15030	TCP4	Leaf development	DN1499_c0_g1_i1	1.8E-02	-
AT2G32280	VCC	Leaf development	DN10816_c0_g1_i1	2.8E-03	4.8E-02
AT1G53230	TCP3	Leaf development	DN1499_c0_g1_i1	1.8E-02	-
AT1G10670	ACLA-1	Leaf development	DN14043_c0_g1_i6	5.6E-08	3.7E-12
			DN3501_c0_g1_i1	9.1E-07	1.0E-03
AT2G31070	TCP10	Leaf development	DN1499_c0_g1_i1	1.8E-02	-
AT4G39400	BIN1	Leaf development	DN18034_c3_g1_i3	3.0E-02	3.1E-02
AT2G42600	PPC2	Leaf development	DN1761_c0_g1_i3	5.4E-05	1.6E-10
			DN1761_c0_g1_i7	2.7E-10	7.4E-09
AT3G11450	ZRF1A	Leaf development	DN2759_c0_g1_i1	1.5E-03	2.5E-02
AT5G28640	AN3	Leaf development	DN4110_c0_g3_i1	2.9E-02	-
AT5G16780	DOT2	Leaf development	DN17075_c0_g1_i4	3.3E-02	-
AT3G08640	RER3	Leaf development	DN7745_c0_g1_i1	-	3.3E-02
			DN3791_c2_g1_i2	4.7E-02	8.7E-04
AT5G05620	TUBG2	Leaf development	DN18798_c0_g4_i1	2.7E-05	6.3E-05
AT5G56030	HSP81.2	Leaf development	DN686_c0_g2_i2	2.7E-12	2.2E-02
			DN686_c0_g3_i1	4.3E-05	6.0E-04
AT5G53660	GRF7	Leaf development	DN13936_c2_g1_i1	5.2E-06	2.5E-07
AT2G28350	ARF10	Leaf development	DN17022_c2_g1_i1	4.1E-05	8.3E-06
			DN17200_c0_g1_i1	3.4E-02	3.7E-02
			DN17353_c0_g1_i1	6.1E-05	4.2E-07

AT5G04810	PPR4	Leaf development	DN8240_c0_g1_i1	-	2.2E-05
AT1G08410	DIG6	Leaf development	DN2443_c0_g1_i1	4.2E-05	2.6E-02
AT1G17980	PAPS1	Leaf development	DN863_c1_g1_i4	5.6E-06	6.1E-08
AT5G10270	CDKC1	Leaf development	DN14557_c1_g2_i1	2.8E-03	4.4E-02
AT5G64960	CDKC2	Leaf development	DN14557_c1_g2_i1	2.8E-03	4.4E-02
AT3G14940	PPC3	Leaf development	DN1761_c0_g1_i3	5.4E-05	1.6E-10
			DN1761_c0_g1_i7	2.7E-10	7.4E-09
AT1G48920	NUC-L1	Leaf development	DN20546_c0_g1_i33	4.5E-07	1.4E-02
			DN20776_c1_g1_i2	2.1E-04	-
			DN670_c0_g1_i10	8.7E-03	-
AT1G13260	EDF4	Leaf development	DN13187_c0_g2_i1	3.0E-02	2.4E-04
AT4G33950	OST1	Leaf development	DN16117_c0_g3_i8	2.2E-02	2.6E-04
AT4G31160	DCAF1	Leaf development	DN3273_c0_g2_i2	5.9E-04	3.5E-02
AT4G00850	GIF3	Leaf development	DN5057_c0_g1_i1	1.1E-03	2.0E-06
AT3G61650	TUBG1	Leaf development	DN18798_c0_g4_i1	2.7E-05	6.3E-05
AT1G01160	GIF2	Leaf development	DN5057_c0_g1_i1	1.0E-03	2.0E-06
AT2G16800	CGF2	Leaf development	DN14886_c4_g2_i1	3.0E-02	-
AT2G28890	PLL4	Leaf development	DN72_c1_g1_i3	3.3E-05	5.9E-03
AT1G70560	CKRC1	Leaf development	DN17357_c0_g1_i9	5.0E-05	1.1E-05
AT4G20360	SVR11	Leaf development	DN18489_c1_g2_i1	1.7E-03	1.4E-11
AT1G15690	AVP1	Leaf development	DN853_c1_g1_i3	1.6E-03	2.3E-07
AT5G58230	MSI1	Leaf development	DN18640_c0_g2_i1	5.0E-02	-
			DN8951_c0_g1_i1	-	1.7E-02
AT4G02440	EID1	Leaf development	DN7960_c0_g1_i1	1.3E-03	8.2E-06
AT1G07630	PLL5	Leaf development	DN72_c1_g1_i3	3.3E-05	5.9E-03
AT4G30340	DGK7	Leaf development	DN3511_c0_g1_i4	2.1E-04	-
AT4G15900	PRL1	Leaf development	DN15335_c1_g3_i2	1.0E-03	1.2E-02
AT4G37650	EAL1	Leaf development	DN15500_c1_g2_i1	3.0E-03	4.0E-03
AT1G56180	VIR3	Leaf development	DN17010_c0_g1_i3	8.9E-03	-
AT3G15380	CTL1	Leaf development	DN405_c1_g1_i1	6.4E-04	1.6E-05
AT2G40300	FER4	Leaf development	DN1831_c0_g1_i1	7.5E-08	4.3E-08
AT1G79440	ENF1	Leaf development	DN3220_c0_g2_i1	2.0E-02	-
AT4G24560	UBP16	Leaf development	DN1421_c0_g2_i3	2.2E-07	1.7E-07
AT1G73590	PIN1	Leaf shape	DN17601_c0_g2_i3	9.3E-05	7.7E-04
AT3G15730	PLD	Leaf shape	DN6193_c0_g1_i6	1.0E-02	-
AT2G34960	CAT5	Leaf margin	DN17698_c1_g1_i1	2.8E-02	3.2E-06
			DN3644_c0_g1_i1	1.2E-02	-
AT2G28680	RmlC-like	Leaf margin	DN19627_c0_g1_i7	1.5E-07	2.3E-13
AT2G39450	MTP11	Leaf margin	DN17749_c0_g1_i10	2.2E-02	-
AT1G70560	CKRC1	Leaf margin	DN17357_c0_g1_i9	5.0E-05	1.1E-05

AT1G52150	CAN	Leaf morphogenesis	DN229_c0_g2_i1	1.9E-03	6.2E-05
			DN229_c0_g3_i1	-	3.0E-02
			DN3600_c0_g1_i3	-	3.0E-02
AT5G39740	RPL5B	Leaf morphogenesis	DN17570_c0_g1_i2	1.0E-02	5.5E-04
AT3G15030	TCP4	Leaf morphogenesis	DN1499_c0_g1_i1	1.8E-02	-
AT1G55250	HUB2	Leaf morphogenesis	DN1008_c0_g1_i1	6.6E-03	4.0E-04
AT2G37630	AS1	Leaf morphogenesis	DN9323_c0_g1_i1	2.0E-07	2.0E-03
AT3G05040	HST1	Leaf morphogenesis	DN3921_c0_g1_i2	3.0E-02	-
AT1G48410	AGO1	Leaf morphogenesis	DN1568_c2_g3_i1	-	2.0E-02
AT1G53230	TCP3	Leaf morphogenesis	DN1499_c0_g1_i1	1.8E-02	-
AT2G23760	SAW2	Leaf morphogenesis	DN15861_c0_g2_i2	6.4E-06	2.2E-09
			DN6003_c0_g1_i1	8.4E-09	2.0E-03
AT3G25520	RPL5A	Leaf morphogenesis	DN17570_c0_g1_i2	1.1E-02	5.0E-04
			DN17570_c0_g1_i5		1.4E-02
AT2G31070	TCP10	Leaf morphogenesis	DN1499_c0_g1_i1	1.0E-02	-
AT4G36870	SAW1	Leaf morphogenesis	DN15861_c0_g2_i2	6.4E-06	2.2E-09
			DN6003_c0_g1_i1	8.4E-09	1.9E-03
AT4G34740	ASE2	Leaf morphogenesis	DN6101_c0_g1_i1	-	2.0E-03
AT2G17040	NAC36	Leaf morphogenesis	DN8530_c0_g1_i1	-	4.5E-03
AT3G20630	UBP14	Leaf morphogenesis	DN1956_c0_g1_i2	3.0E-04	2.0E-03
AT1G14400	UBC1	Leaf morphogenesis	DN15508_c1_g1_i2	2.0E-02	-
AT1G01510	AN	Leaf morphogenesis	DN2861_c0_g1_i1	2.0E-02	-
AT4G00100	PFL2	Leaf morphogenesis	DN1650_c0_g1_i1	3.0E-03	9.0E-03
AT5G08370	AGAL2	Leaf morphogenesis	DN2943_c0_g1_i2	5.0E-03	6.0E-03
AT4G03550	EED3	Leaf morphogenesis	DN0_c0_g1_i2	8.0E-03	1.2E-05
AT3G53020	RPL24	Leaf morphogenesis	DN17975_c0_g1_i1	-	4.0E-02
AT4G29040	RPT2A	Leaf morphogenesis	DN13563_c1_g1_i3	1.0E-02	1.0E-02
AT1G26440	UPS5	Leaf lamina	DN490_c0_g1_i12	8.5E-07	9.1E-06
AT2G03530	UPS2	Leaf lamina	DN490_c0_g1_i12	8.5E-07	9.1E-06
AT2G47220	DUF5	Leaf lamina	DN19824_c2_g1_i4	4.0E-03	-
AT2G26540	DUF3	Leaf lamina	DN13523_c0_g1_i1	5.0E-03	6.6E-04
AT5G08000	PDCB2	Leaf lamina	DN15838_c0_g4_i1	8.5E-25	2.9E-16
AT5G58787	IRP4	Leaf lamina	DN14981_c4_g1_i1	1.1E-02	6.9E-07
			DN17802_c2_g1_i11	8.0E-03	1.8E-02
AT5G61130	PDCB1	Leaf lamina	DN15838_c0_g4_i1	8.5E-25	2.9E-16
AT5G38030	DTX30	Leaf lamina	DN6970_c0_g2_i1	2.0E-02	-

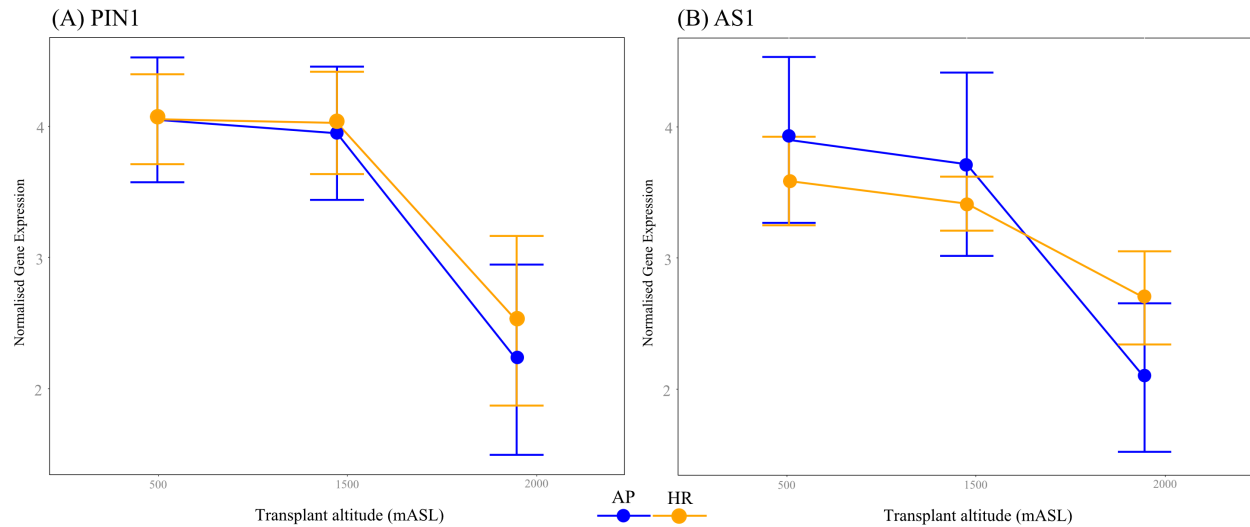
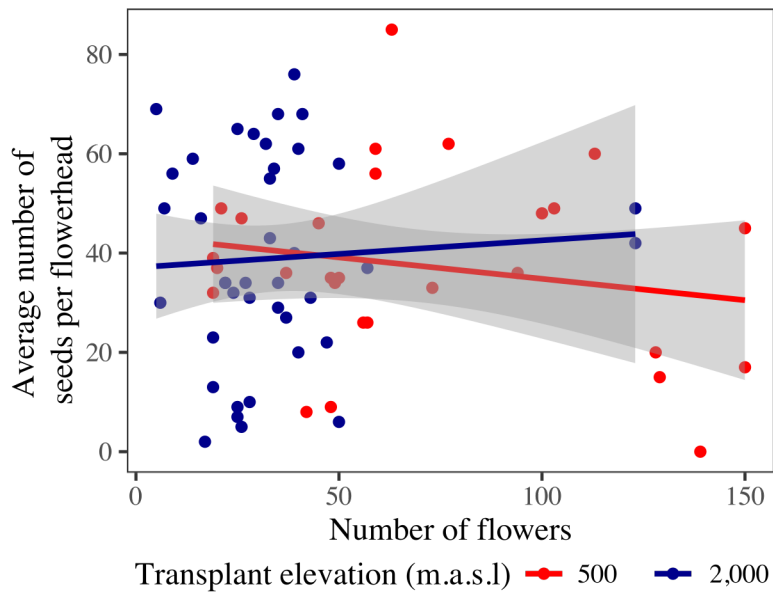


Fig. S5 Comparing elevational changes in mean expression for the *AP* (blue) and *HR* (orange) genotypes of *S. chrysanthemifolius* that are orthologs for two genes of known function in *Arabidopsis*: **(a)** *PIN1* gene that functions in leaf development; and **(b)** *AS1* gene that functions in leaf shape. The mean expression for each gene is represented by a circle and credible intervals represent 95% confidence intervals.

Methods S1. Comparing fitness as the number of flowers versus seed production

In a previous transplant that studied *S. chrysanthemifolius* (Walter *et al.*, 2022), we compared the number of flowers to the proportion of seeds produced. For randomly selected individuals transplanted at the elevational extremes (500 m $n = 28$; 2,000 m $n = 40$), we counted the number of flowers and then collected mature seed heads on two sampling dates. Viable seeds were considered those that were large, brown and round; unviable seeds were those that were thin, empty and generally white. We used a linear mixed effects model implemented with 'lme4' (Bates *et al.*, 2015) to test whether the number of flowers was associated with seed set. We included seed set as the response variable, and transplant site and number of flowers (and their interaction) as the fixed effects. Block within transplant site was the only random effect. We predicted that if plants that produced a large number of flowers also produced a large number of seed, then we would observe no association between the number of flowers produced and the average seed set per flower. This would suggest that the number of flowers provides a good estimate of total fitness because plants that produce more flowers would also produce more seeds. We found that the interaction between the number of flowers and transplant site was not significant ($\chi^2(1) = 0.7856, P = 0.3754$), suggesting that the association between flower number and seed production was high and consistent across elevation (**Fig. A**).

We then used the Kenwood-Roger approach, which is used to test the significance of fixed effects, to test whether the number of flowers was associated with seed set. As predicted, we found no significant effect of the number of flowers on average seeds produced per flower ($F_{1,27.1} = 0.2089, P = 0.6513$), indicating that the number of seeds produced per inflorescence was similar for all plants. The number of flowers therefore provides a good representation for the total number of seeds produced for each plant, and provides a robust estimate of total fitness.



Methods S1 Fig. A The number of flowers produced by any given *S. chrysanthemifolius* plant was not correlated with seed set (i.e., the number of seeds produced *per flower*), and this was consistent for both transplant sites. Therefore, the number of seeds produced per flower is consistent regardless of the number of flowers produced, suggesting that plants that produce more flowers also produce more seeds, and that flower number is likely to be highly correlated with seed set.

Methods S2. RNA extraction, sequencing and transcriptome assembly

Choosing genotypes

Because our collection of young leaves for RNA samples had to be completed before the winter snow arrived, we were restricted to choosing genotypes before the flowers of all cuttings were counted. After flowers were counted for two clones of each genotype at each transplant site, we estimated genetic variation for fitness as the among-genotype variance (i.e. among the individuals in the crossing design) at each transplant site, and the covariance between transplants sites (see equation 1). We then chose the 15 genotypes with the highest (*AP* genotypes for ‘*Adaptive Potential*’) and the 15 genotypes with the lowest (*HR* genotypes for ‘*Home Range*’) relative fitness at 2,000 m. After fitness was quantified for all cuttings, we repeated the analysis for choosing the genotypes (this time with all the fitness data included), and from the sampled genotypes we chose the six *AP* genotypes and six *HR* genotypes for gene expression analysis that maintained the strongest fitness differences at 2,000 m (**Fig. S2a**). Importantly, chosen genotypes also represented changes in genetic variance in fitness, whereby sires of the chosen genotypes exhibited similar fitness responses to elevation (**Fig. S2b**).

RNA extraction and sequencing

For each clone, we homogenized all collected tissue and performed RNA extraction using a Qiagen RNeasy kit with β -mercaptoethanol added to the lysis buffer and included a DNase digestion step. We measured RNA purity and concentration using a Nanodrop ND1000 spectrophotometer and Qubit fluorometer. All sequencing and library preparation was performed at the Oxford Genomics Centre, The Wellcome Centre for Human Genetics, Oxford (UK). For each selected genotype, total RNA from a single individual was sequenced to produce 150bp reads using an Illumina NovaSeq6000 platform. For each individual, a small region close to the

3' end of each transcript was sequenced to produce 75bp reads using a Lexogen QuantSeq library preparation and Illumina NextSeq500 platform (Moll *et al.*, 2014).

Reference Transcriptome Assembly

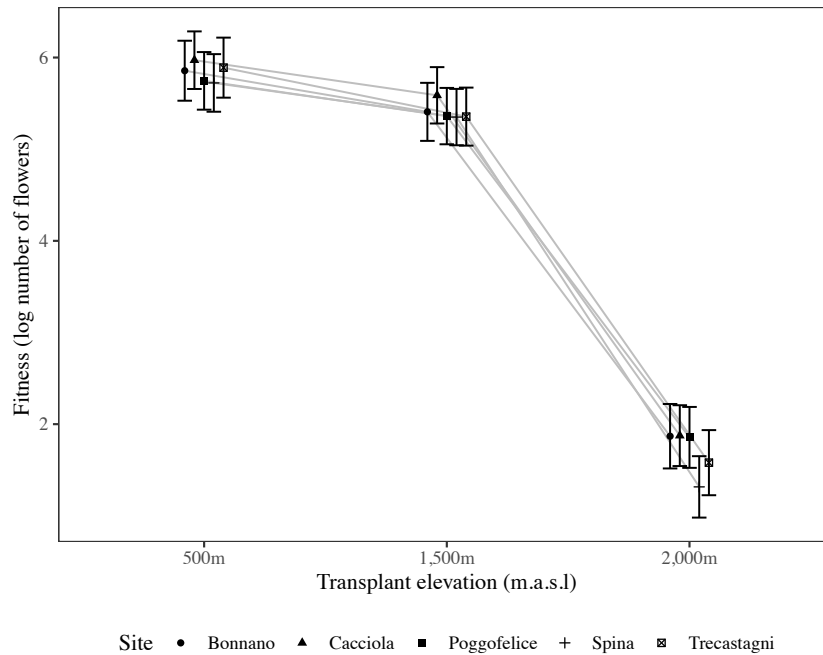
RNAseq of total RNA produced on average 28.75 million reads per sample. The 3' sequencing produced on average 5.46 million reads per sample. Only samples that produced more than 1 million reads (n = 98) were included in downstream analyses. Quality assessment and trimming of all reads was performed using TrimGalore v0.6 (Phred quality cut-off = 20). Trimmed reads from the total RNAseq for each genotype were combined and a single reference transcriptome was *de novo* assembled in Trinity v2.8.4 (Haas *et al.*, 2013). To reduce transcript and isoform redundancy, we filtered the transcriptome using the EvidentialGene pipeline (minimum sequence length = 400 nucleotides) (Gilbert, 2019) and contaminating sequences were removed using the MCSC Decontamination pipeline (filter = Viridiplantae) (Lafond-Lapalme *et al.*, 2017). The reference transcriptome contained 29,224 transcripts with an n50 of 2,030 nucleotides. The reference transcriptome was annotated using the pipeline (Bryant *et al.*, 2017). Nucleotide sequences were used to perform a *Diamond blastx* search and translated amino acid sequences were used to perform a *Diamond blastp* search, each of the *UniProt* database with a 1×10^{-20} cut-off. This resulted in 22,335 unique annotations, and on average 1.06 annotations per transcript.

Methods S3. Contribution of site variance to estimates of genetic variance

Our estimates of genetic variance are taken from a population of *S. chrysanthemifolius* that we randomly sampled across five sites. If sites were to be very different, either due to local adaptation or genetic drift, then our estimates of genetic variance could be conflated by differences among sites. Although the interpretation of genetic variance with respect to the species remains the same because our estimates of genetic variance represent the adaptive potential for the randomly sampled parental generation from the broader population.

To ensure that site differences did not conflate our estimates of genetic variance we took two approaches: First, we tested for local adaptation using fitness data (collected using the same methods as the current study) from a previous experiment that transplanted individuals from all five sites at the same elevations (Walter *et al.*, 2022). We found no evidence of local adaptation (**Fig. B**), suggesting that the sites have not undergone adaptive divergence within their home range.

Second, we re-analysed the fitness data from equation 1 in the main text, but included an additional random effects term (c_p) that estimates the variance among crosses and includes crosses conducted within sites (e.g. Spina×Spina) and among sites (e.g. Spina×Bonnano). We found that differences among sampling sites only accounted for a small proportion (0.5%) of the total variance in fitness compared to additive genetic variance estimated from the sire component (9.3%) (**Table A**). These results, combined with no evidence of local adaptation among sites (**Fig. B**), suggest that the five sampling sites are part of the same inter-connected population.



Methods S3 Fig. B Fitness was similar for the genotypes of all five sites when transplanted as cuttings in 2019. This suggests that the five sites are not locally adapted and that they represent part of the same population. The experiment is described in detail in Walter *et al.* (2022).

Methods S3 Table A Estimates of variance for each random component in equation 1, but also including the extra ‘Site’ component. Additive genetic variance is estimated as four times the sire variance.

Component	500 m	1,500 m	2,000 m
Sire	0.008	0.005	0.031
Dam	0.015	0.003	0.012
Genotype	0.078	0.051	0.111
Site	0.007	0.002	0.007
Block	0.371	0.467	0.554
Residual	0.545	0.379	0.614

Methods S4. Relating phenotypic traits to the elevational gradient

Phenotypic variances (variance among all plants) tended to decrease with altitude, except for flavonol content, which increased in variance (**Table B**). Using analysis of variance on each trait independently, we tested whether differences among the 314 genotypes in the breeding design described more variance than among clones within genotypes. We also included transplant site and experimental block nested within transplant site. All traits showed greater variance among genotypes than among clones within genotypes (leaf area: $F_{313,4592} = 2.963$, $P < 0.0001$; leaf complexity: $F_{313,4592} = 11.761$, $P < 0.0001$; number of indents: $F_{313,4592} = 8.962$, $P < 0.0001$; SLA: $F_{313,4592} = 4.731$, $P < 0.0001$; Flavonol content: $F_{313,4745} = 3.851$, $P < 0.0001$). This meant that differences among the 314 genotypes accounted for >20% of the total variance in each trait (leaf area = 35.8%, leaf complexity = 51.3%, number of indents = 54.7%, SLA = 51.1% and flavonol content = 20.1%). Therefore, differences among genotypes were significant and multiple clones provided a reliable representation of the response of each genotype to environmental variation across elevation.

Methods S4 Table B Total phenotypic variances (variances among all clones) for each trait at each elevation.

	Area	Leaf complexity	Number of indents	SLA	Flavonol
500 m	0.255	0.125	0.032	0.045	0.082
1,500 m	0.145	0.080	0.041	0.048	0.102
2,000 m	0.050	0.063	0.027	0.040	0.124

References

- Bates D, Machler M, Bolker BM, Walker SC. 2015.** Fitting linear mixed-effects models using lme4. *Journal of Statistical Software* **67**(1): 1-48.
- Bryant DM, Johnson K, DiTommaso T, Tickle T, Cougar MB, Payzin-Dogru D, Lee TJ, Leigh ND, Kuo TH, Davis FG, et al. 2017.** A tissue-mapped Axolotl de novo transcriptome enables identification of limb regeneration factors. *Cell Reports* **18**(3): 762-776.
- Gilbert DG. 2019.** Longest protein, longest transcript or most expression, for accurate gene reconstruction of transcriptomes? *bioRxiv*: 829184.
- Haas BJ, Papanicolaou A, Yassour M, Grabherr M, Blood PD, Bowden J, Couger MB, Eccles D, Li B, Lieber M. 2013.** De novo transcript sequence reconstruction from RNA-seq using the Trinity platform for reference generation and analysis. *Nature protocols* **8**(8): 1494.
- Lafond-Lapalme J, Duceppe M-O, Wang S, Moffett P, Mimee B. 2017.** A new method for decontamination of de novo transcriptomes using a hierarchical clustering algorithm. *Bioinformatics* **33**(9): 1293-1300.
- Moll P, Ante M, Seitz A, Reda T. 2014.** QuantSeq 3' mRNA sequencing for RNA quantification. *Nature Methods* **11**(12): 972.
- Walter GM, Clark J, Cristaudo A, Nevado B, Catara S, Paunov M, Velikova V, Filatov D, Cozzolino S, Hiscock SJ, et al. 2022.** Adaptive divergence generates distinct plastic responses in two closely related *Senecio* species. *Evolution* **76**(6): 1229-1245.